CHAPTER 8

# Convection

Convection is a kind of fluid flow driven by internal buoyancy. In general, the buoyancy that drives convection derives from horizontal density gradients. In the mantle, the main sources of density gradients are horizontal thermal boundary layers. Convection is driven when the buoyancy (positive or negative) of a thermal boundary layer causes it to become unstable, so that fluid from it leaves the boundary of the fluid and rises or falls through the interior of the fluid. This statement may seem to be labouring the obvious, but there has been a lot of confusion about the nature of mantle convection, and much of this confusion can be avoided by keeping these basic ideas clearly in mind.

In general the buoyancy driving convection may be of thermal or compositional origin. We will be concerned mainly with thermal buoyancy, but compositional buoyancy is also important in the mantle. It is best to consider first thermal convection, that is convection driven by thermal buoyancy. Some aspects of compositional buoyancy will be considered in Chapter 14.

Here I describe sources of buoyancy, give a simple example of thermal convection, and show how there is an intimate relationship between convection and the surface topography that it produces. This establishes some basic concepts that will be applied more explicitly to the mantle in subsequent chapters.

In the course of doing this, I show how convection problems scale, how the Rayleigh number encapsulates this scaling, why convection occurs only if the fluid is heated or cooled strongly enough, and how the mode of heating (from below or internally) governs the nature of the thermal boundary layers. In principle there may be two thermal boundary layers in a fluid layer, one at the top and one at the bottom, or there may be only one, depending on the way the fluid is heated and cooled.

## 8.1 Buoyancy

Buoyancy arises from gravity acting on density differences. Technically, buoyancy is used to describe a *force*. Thus it is not the same as a density difference. Rather, it is the product of a density difference, $\Delta\rho$, a volume, $V$, and the gravitational acceleration, $g$:

$$B = -gV\Delta\rho = -g\Delta m \tag{8.1.1}$$

where $\Delta m$ is the mass anomaly due to a volume $V$ with a density difference $\Delta\rho = \rho_V - \rho$ from its surroundings. The minus is used because, in common usage, buoyancy is positive upwards, whereas gravity and weight are positive downwards. Thus for a density excess, $\Delta\rho$ is positive and $B$ is negative, that is downwards.

It is buoyancy rather than just density difference that is important in convection. A large density difference within a small volume may be unimportant. For example, you might expect intuitively that a steel ball-bearing, 1 cm in diameter, embedded in the mantle would not sink rapidly to the core, despite a density difference of over 100%. On the other hand, a plume head with a density contrast of only about 1% would have a significant velocity if its diameter were 1000 km, as we saw in Section 6.8.

With thermal buoyancy, density differences arise from thermal expansion. This is described by

$$\rho = \rho_0[1 - \alpha(T - T_0)] \tag{8.1.2}$$

where $\rho$ is density, $\alpha$ is the volume coefficient of thermal expansion, $T$ is temperature, and $\rho_0$ is the density at a reference temperature $T_0$. With $\alpha$ typically about $3 \times 10^{-5}/^{\circ}\mathrm{C}$ (Table 7.3), a temperature contrast of 1000 °C gives rise to a density contrast of about 3%. In the lower mantle, where $\alpha$ may be only about $1 \times 10^{-5}/^{\circ}\mathrm{C}$ due to the effect of pressure, the corresponding density difference would be only about 1%.

There are some density differences in the earth larger than these thermal density differences, and these are due to differences in chemical or mineralogical composition. For example the oceanic crust has a density of about $2.9\,\mathrm{Mg/m^3}$, compared with an upper mantle density of about $3.3\,\mathrm{Mg/m^3}$, so it has a density deficit of about $400\,\mathrm{kg/m^3}$ or 12%. The total density change through the mantle transition zone is about 15%. Much or all of this is believed to be due to pressure-induced phase transformations of the mineral assemblage (Chapter 5), and so it is not necessarily a source of buoyancy. However, locally all of the density differences associated

with particular transformations may be operative because the depth of the transformation is changed by temperature, as was discussed in Chapter 5. Apart from this, if the density increase through the transition zone is not all due to phase transformations, the maximum that could be attributed to a difference between the composition of the upper mantle and the lower mantle is a small percentage, according to the seismological and material property constraints discussed in Chapter 5.

It is useful to have some idea of the magnitudes of buoyancies of various objects. For example, a ball bearing would exert a buoyancy force of about $-0.02\,\mathrm{N}$ (taking buoyancy to be positive upwards), while a plume head 1000 km in diameter with a temperature difference of 300 °C would have a buoyancy of about $2 \times 10^{20}\,\mathrm{N}$. Subducted lithosphere extending to a depth of 600 km exerts a buoyancy of about $-40\,\mathrm{TN}$ per metre of oceanic trench, that is per metre horizontally in the direction of strike of the subducted slab.

If the subducted lithosphere extended to the bottom of the mantle, about 3000 km in depth, its buoyancy would be about $-200\,\mathrm{TN/m}$. Comparing this with a plume head, it takes a piece of subducted lithosphere about 1000 km wide and 3000 km deep to equal in magnitude the buoyancy of a plume head. While this may make plume heads seem to be very important, you should bear in mind that the total length of oceanic trenches is over 30 000 km. Thus, while the buoyancy of a plume head is impressive, it is still small compared to the total buoyancy of subducted lithosphere.

The crustal component of subducted lithosphere undergoes a different sequence of pressure-induced phase transformations than the mantle component, and as a result it is sometimes less dense and sometimes denser than the surrounding mantle, with the difference usually no more than about $200\,\mathrm{kg/m^3}$ (Section 5.3.4). Even if it had the same density difference, say $-100\,\mathrm{kg/m^3}$, extending throughout the mantle, its thickness is only about 7 km and its total contribution to slab buoyancy would be only about 20 TN/m, compared with the slab thermal buoyancy of $-200\,\mathrm{TN/m}$. This suggests that normally the crustal component of subducted lithosphere does not substantially affect the slab buoyancy. However, if the subducted lithosphere is young, so that its negative thermal buoyancy is small, the crustal buoyancy may be more important. This may have been more commonly true at earlier times in earth history. These possibilities will be taken up again in Chapter 14.

The very large range of the magnitudes of buoyancies of the various objects just considered serves to emphasise that we must

consider the volume occupied by anomalous density, not just the magnitude of the density anomaly itself.

## 8.2 A simple quantitative convection model

We are now ready to consider a convection model that is simple in concept but goes to the heart of plate tectonics and its relationship with mantle convection. The approach was first used by Turcotte and Oxburgh in 1967 [1]. At that time plate tectonics was only just beginning to gain acceptance amongst geophysicists. I give a simplified version here. A more detailed version is given by Turcotte and Schubert [2], p. 279. I also acknowledge that it is only within the last five years or so that numerical models have become substantially superior to Turcotte and Oxburgh's approximate analytical model. Such is the power of capturing the simple essence of a problem.

Consider plates on a viscous mantle, as sketched in Figure 8.1a. The plates comprise a thermal boundary layer, within which the temperature changes from the surface temperature to the temperature within the interior of the mantle. Because the plates are cold, they are denser and prone to sink: they have negative buoyancy. In Figure 8.1a, one plate is depicted as subducting, and we presume here that it is sinking under its own weight. As the subducted part sinks, it drags along the surrounding viscous mantle with it. The motion of the plate is resisted by the viscous stresses accompanying

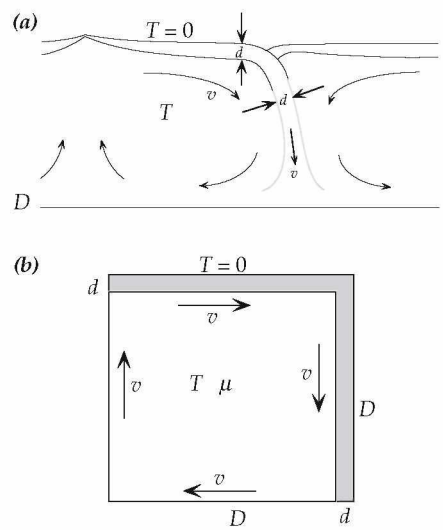


Figure 8.1. (a) Sketch of flow driven by a subducting plate. (b) Idealised form of the situation in (a).

this mantle flow. The viscous stresses are proportional to velocity. This permits an equilibrium to develop between the opposing forces: the velocity adjusts until the resistance balances the buoyancy.

Our approach is based on the same principle as that used in Chapter 6 when we considered flow down a pipe that is driven by the fluid's own weight, and the rise of a buoyant sphere. In each case, there was a balance between a buoyancy force and a viscous resistance. The system achieves balance by adjusting its velocity until the viscous resistance balances the buoyancy. This balance is stable, in the sense that a change in the velocity will induce an imbalance of the forces that will quickly return the velocity to its equilibrium value. However, we should remember that the motions are so slow in the mantle that accelerations and momenta are quite negligible, and the forces are essentially in balance at every instant, though their magnitudes may slowly change in concert.

Let us make a simple dimensional estimate of the balance between buoyancy and viscous forces, in the same way as we did for the buoyant sphere in Chapter 6. Here, because the two-dimensional sketch is assumed to be a cross-section through a structure that extends in the third dimension, the forces will be calculated per unit length in the third dimension. Let us also simplify the geometry into that depicted in Figure 8.1b.

First consider the buoyancy of the lithosphere descending down the right side of the box. Assume that this lithosphere simply turned and descended, preserving its thickness and temperature profile. From the basic formulas (8.1.1) and (8.1.2), the buoyancy is

$$B = g \cdot Dd \cdot \rho\alpha\Delta T$$

where $\Delta T$ is the average difference in temperature between the descending lithosphere and the fluid interior. This is approximately $\Delta T = -T/2$, where $T$ is the temperature of the interior fluid. (We used the same approximation in estimating the subsidence of oceanic lithosphere in Section 7.4). Thus

$$B = -g \cdot Dd\rho\alpha T/2 \tag{8.2.1}$$

If we want to evaluate this expression, we can independently estimate the values of all quantities except the thickness, $d$, of the lithosphere upon subduction. This is just the thickness of the layer that has cooled by conduction of heat to the surface, as we considered in Section 7.3. It is determined by the amount of time the subducting piece of lithosphere spent at the surface. This time is

$t = D/v$. According to the discussion of thermal diffusion in Chapter 7, the thickness of the layer from which heat has diffused is approximated by

$$d = \sqrt{\kappa t} = \sqrt{\kappa D/v} \tag{8.2.2}$$

where $\kappa$ is the thermal diffusivity. So we have an expression for $d$, but now it includes the still-unknown quantity $v$. We will see below how to deal with it.

Now consider the viscous resistance. As with our rough estimate for a buoyant sphere (Section 6.8.1), we estimate the viscous stresses from a characteristic velocity gradient. In this case, the velocity changes from $v$ to $-v$ across the dimensions of the box, so a representative velocity gradient is $2v/D$. The resisting viscous stress $\sigma$ acting on the side of the descending slab is then

$$\sigma = \mu \cdot 2v/D$$

This is a force per unit area. We get the force per unit length (in the third dimension) by multiplying $\sigma$ by the vertical length, $D$, of the slab:

$$R = D\sigma = D \cdot 2\mu v/D = 2\mu v \tag{8.2.3}$$

The buoyancy and resistance are balanced when $B + R = 0$. From (8.2.1) and (8.2.3), this occurs when

$$v = -g \cdot Dd\rho\alpha T/4\mu \tag{8.2.4}$$

This expression for $v$ also involves $d$. We can combine Equations (8.2.2) and (8.2.4) to solve for the two unknowns $v$ and $d$. The result is

$$v = D\left(\frac{g\rho\alpha T\sqrt{\kappa}}{4\mu}\right)^{2/3} \tag{8.2.5}$$

Using $D = 3000\,\text{km}$, $\rho = 4000\ \text{kg/m}^3$, $\alpha = 2 \times 10^{-5}/^\circ\text{C}$, $T = 1400\,^\circ\text{C}$, $\kappa = 10^{-6}\,\text{m}^2/\text{s}$ and $\mu = 10^{22}\,\text{Pa s}$, this yields $v = 2.8 \times 10^{-9}\,\text{m/s} = 90\,\text{mm/a}$. This is quite a good estimate of the velocity of the faster plates.

Other quantities can be estimated from these results. From Equation (8.2.2), the thickness of the lithosphere is 33 km. This is of the same order of magnitude as the observed oceanic lithosphere, though about a factor of two too small. If we had used the more accurate estimate of $d = 2\sqrt{(kt)}$ that is obtained from the

error function solution for the cooling lithosphere (Equation (7.3.3)), we would have obtained 66 km. Also our estimate of the time the lithosphere spent cooling at the surface is a bit small, because we assumed implicitly in Figure 8.1b that the plate is only as wide as the mantle is deep, that is about 3000 km. At a velocity of 90 mm/a = 90 km/Ma, the plate will be only 33 Ma old when it subducts. Observed lithosphere of this age is about 60 km thick. If the box were longer, the plate would be older and thicker. This problem is left as an Exercise.

The surface heat flux, $q$, can also be estimated from the temperature gradient through the boundary layer: $q = KT/d$, where $K$ is the thermal conductivity. Using $K = 3\,\mathrm{W/m\,K}$, this gives $q = 130\,\mathrm{mW/m^2}$. This compares with an observed heat flux of about $90\,\mathrm{mW/m^2}$ for lithosphere of this age, and a mean heat flux of about $100\,\mathrm{mW/m^2}$ for the whole sea floor.

The point of these estimates is not that they are not very accurate, but that they are of the right order of magnitude. In the absence of the simple theory developed above, one could not make a sensible estimate even of the orders of magnitude to be expected. Given the crudity of the approximations made, the agreement within about a factor of two is very good, perhaps better than is really justified.

The agreement of these estimates with observations suggests that we have a viable theory for mantle convection that explains why plates move at their observed velocities. Think about the significance of that statement for a moment. Plate tectonics is recognised as a fundamental mechanism driving geological processes. Within a few pages, with some simple physics and simple approximations, we have produced a theory that is consistent with some primary observations of plate tectonics (their velocities, thicknesses and heat fluxes). We thus have a candidate theory for the underlying mechanism for a very wide range of geological processes. We will be further testing the viability (and sufficiency) of this theory through much of the rest of this book.

## 8.3 Scaling and the Rayleigh number

The approximate theory just developed yields not only reasonable numerical estimates of observed quantities, but also information on how these quantities should scale. Thus, for example, according to Equation (8.2.5), if the viscosity were a factor of 10 lower at some earlier time in earth history, the plate velocities would not be 10 times greater, but $10^{2/3} = 4.6$ times greater. Similarly, we can combine Equations (8.2.2) and (8.2.5) and deduce that

$$\left(\frac{D}{d}\right)^3 = \frac{g\rho\alpha T D^3}{4\kappa\mu} \tag{8.3.1}$$

This implies that the boundary layer thickness would have been 2.15 times less (15 km) and the heat flow 2.15 times higher (275 mW/m$^2$) with a viscosity 10 times lower.

Equation (8.3.1) is written in this particular form to make a more general point. The left side involves a ratio of lengths, and it is therefore dimensionless. One can work through the dimensions of the right side and confirm that it is also dimensionless, as it should be. This particular, rather arbitrary looking, collection of constants actually encapsulates the scaling properties that we have just looked at, and others besides. In fact it encapsulates many of the scaling properties of convection in a fluid layer in general, not just the mantle convection we are concerned with here. For this reason it has been recognised by fluid dynamicists as having a fundamental significance for all forms of thermal convection. It was Lord Rayleigh who first demonstrated this, and this dimensionless combination (without the numerical factor) is known as the Rayleigh number in his honour. It is usually written

$$Ra = \frac{g\rho\alpha T D^3}{\kappa\mu} \tag{8.3.2}$$

For the mantle, using values used in the last section, we can estimate that $Ra \approx 3 \times 10^6$.

We can see explicitly the way in which the Rayleigh number encapsulates the scaling properties by rewriting the above results in terms of $Ra$. Thus, from Equation (8.3.1),

$$d/D \sim Ra^{-1/3} \tag{8.3.3}$$

where '$\sim$' implies proportionality and 'of the order of'. The ratio $d/D$ is obviously dimensionless also, and we can view this ratio as a way of scaling $d$, relative to a length scale that is characteristic of the problem, namely the depth of the fluid layer, $D$. Similarly, from Equation (8.2.5)

$$v(D/\kappa) \equiv v/V \sim Ra^{2/3} \tag{8.3.4}$$

The dimensions of $\kappa$ are (length$^2$/time), so the ratio $\kappa/D$ has the dimensions of velocity. We can thus regard $V = \kappa/D$ as a velocity scale characteristic of the problem. Then Equation (8.3.4) shows how the actual flow velocity $v$ relates to the velocity scale $V$ derived

from the geometry of the problem and the properties of the material.

Fluid dynamicists are enamoured of these dimensionless ratios, for the very good reason that they encapsulate important scaling information, and they have named lots of them after people. Thus the combination $vD/\kappa$ is called the Peclet number, written $Pe$:

$$Pe \equiv vD/\kappa = v/V \tag{8.3.5}$$

Then Equation (8.2.5) reduces to $Pe \sim Ra^{2/3}$. Using values from the last section, we can estimate that for the mantle $Pe \approx 9000$.

I will not go through an exhaustive catalogue of these dimensionless numbers here, but a couple of further examples are worth noting. First, it is instructive to combine the scaling quantities $V$ and $D$ to define a characteristic time:

$$t_\kappa \equiv D/V = D^2/\kappa \tag{8.3.6}$$

From Chapter 7, this can be recognised as a diffusion time scale. It is an estimate of the time it would take the fluid layer to cool significantly by thermal diffusion, that is by conduction, in the absence of convection. Compare this with a time scale that is more characteristic of the convection process: $t_v = D/v$. This is the time it takes the fluid to traverse the depth of the fluid layer at the typical convective velocity, $v$, so it can be called the transit time. From Equations (8.3.4) and (8.3.6),

$$t_v = D/v = t_\kappa Ra^{-2/3} \tag{8.3.7}$$

If $Ra = 3 \times 10^6$, then $t_v = 5 \times 10^{-5} t_\kappa$. Thus if $Ra$ is large, $t_v$ is much smaller than $t_\kappa$, reflecting the fact that, at high Rayleigh numbers, convection is a much more efficient heat transport mechanism than conduction.

Actually Equation (8.3.7) indicates that $t_\kappa$ is not a very useful time scale for convection processes, since it is a measure of thermal conduction. A better one would be that given by the second equality in Equation (8.3.7). Thus we can define a time scale characteristic of convection as

$$t_v \equiv (D^2/\kappa)Ra^{-2/3} \tag{8.3.8}$$

To complete this discussion of scaling for now, we will return to the heat flux, estimated in the last section from $q = KT/d$. Using Equation (8.3.3), you can see that

$$q = (KT/D)Ra^{1/3} \tag{8.3.9}$$

Again you can recognise $(KT/D)$ as a scaling quantity. In this case it is the heat that would be conducted across the fluid layer (not the boundary layer) if the base were held at the temperature $T$ and the surface at $T = 0$. In other words, it is the heat that would be conducted in the steady state in the absence of convection. Denote this as $q_K$. The ratio $q/q_K$ is known as the Nusselt number, denoted as $Nu$:

$$Nu \equiv q/q_K = qD/KT \tag{8.3.10}$$

Then Equation (8.3.9) reduces to

$$Nu \sim Ra^{1/3} \tag{8.3.11}$$

Thus the Nusselt number is a direct measure of the efficiency of convection as a heat transport mechanism relative to conduction. For the mantle, $Nu \approx 100$. In other words, mantle convection is about two orders of magnitude more efficient at transporting heat than conduction would be.

## 8.4 Marginal stability

Traditional treatments of convection often begin with an analysis of marginal stability, which is the analysis of a fluid layer just at the point when convection is about to begin. This approach reflects the historical development of the topic, and the fact that the mathematics of marginal stability has yielded analytical solutions. The mantle is far from marginal stability, as we will see, and so I began the topic of convection differently, with the more directly relevant 'finite amplitude' convection problem.

Nevertheless the marginal stability problem gives us some important physical insights into convection and the Rayleigh number. However, many treatments of it give long and intricate mathematical derivations and do not always make the physics clear. I will err in the other direction, keeping the mathematics as simple as possible and endeavouring to clarify the physics.

The marginal stability problem arises from the fact that, for a fluid layer heated uniformly on a lower horizontal boundary, there is a minimum amount of heating below which convection does not occur. If the temperature at the bottom is initially equal to the temperature at the top, then of course there will be no convection. Now if the bottom temperature is slowly increased, still there will

be no convection, until some critical temperature difference is reached, at which point slow convection will begin. At this point, the fluid layer has just become unstable and begins to overturn. The transition, just at the point of instability, is called marginal stability. Lord Rayleigh [3] was the first to provide a mathematical analysis of this. He showed that marginal stability occurs at a critical value of the Rayleigh number. The critical value depends on the particular boundary conditions and other geometric details, but is usually of the order of 1000. The mathematical analysis of marginal stability is reproduced by Chandrasekhar [4] and by Turcotte and Schubert [2] (p. 274).

Consider the two layers of fluid sketched in Figure 8.2. The lower layer is less dense, and the interface between them has a bulge of height $h$ and width $w$. Take $h$ to be quite small. This bulge is buoyant relative to the overlying fluid, and its buoyancy is approximately

$$B = g\Delta\rho wh$$

per unit length in the third dimension. Its buoyancy will make it grow, so that its highest point rises with some velocity $v = \partial h/\partial t$, and its growth will be resisted by viscous stresses.

The viscous resistance will have different forms, depending on whether the width of the bulge is smaller or larger than the layer depth $D$. If $w \ll D$, the dominant shear resistance will be proportional to the velocity gradient $v/w$. The resisting force is then

$$R_s = \mu(v/w)w = \mu v = \mu\partial h/\partial t$$

where $v/w$ is a characteristic strain rate and the subscript 's' denotes small $w$. Equating $B$ and $R_s$ to balance the forces yields

$$\frac{\partial h}{\partial t} = \frac{g\Delta\rho w}{\mu}h \tag{8.4.1}$$

which has the solution

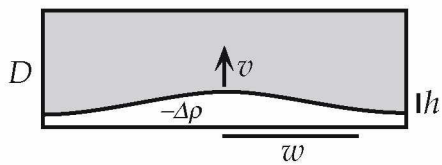


Figure 8.2. Sketch of two layers of fluid with the denser fluid above and with an undulating interface that is unstable.

$$h = h_0 \exp(t/\tau_s) \tag{8.4.2}$$

where $h_0$ is a constant and

$$\tau_s = \frac{\mu}{g\Delta\rho w} \tag{8.4.3}$$

In other words, the bulge grows exponentially with a time constant $\tau_s$, because the interface is unstable: the lighter fluid wants to rise to the top. This kind of instability is called the Rayleigh–Taylor instability. It occurs regardless of the reason for the density difference between the two fluids.

Notice that $\tau_s$ gets smaller as $w$ gets bigger. That is, broader bulges grow more quickly. However, there is a limit to this: when the width of the bulge is comparable to the depth, $D$, of the fluid layer, the top boundary starts to interfere with the flow and to increase the viscous resistance. If $w$ is much larger than $D$, then the dominant viscous resistance comes from horizontal shear flow with velocity $u$ along the layer. By conservation of mass, $uD = vw$. The characteristic velocity gradient of this shear flow is then $u/D = vw/D^2$. The resulting shear stress acts across the width $w$ of the bulge, so the resisting force in this case is

$$R_l = \mu(u/D)w = \mu v w^2/D^2$$

where subscript 'l' denotes large $w$. Balancing $R_l$ and $B$ then yields

$$\frac{\partial h}{\partial t} = \frac{g\Delta\rho D^2}{\mu w} h \tag{8.4.4}$$

which has the same form as Equation (8.4.1) except for the constants. It also has the same form of exponentially growing solution (Equation (8.4.2)), but with a different time scale $\tau_l$:

$$\tau_l = \frac{\mu w}{g\Delta\rho D^2} \tag{8.4.5}$$

Notice here that $\tau_l$ gets *bigger* for larger $w$, whereas $\tau_s$ gets smaller, and their values are equal when $w = D$. We have considered the two extreme cases $w \ll D$ and $w \gg D$. As $w$ approaches $D$ from either side, the time scale of the growth of the instability gets smaller. This implies that the time scale is a minimum near $w = D$. In other words, a bulge whose horizontal scale is $w = D$ is the fastest growing bulge, and its growth time scale is

$$\tau_{RT} = \frac{\mu}{g\Delta\rho D} \tag{8.4.6}$$

where the subscript 'RT' connotes the Rayleigh–Taylor time scale. A more rigorous analysis that yields this result is given by Turcotte and Schubert [2] (p. 251). The implication of this result is that if there are random small deviations of the interface from being perfectly horizontal, deviations that have a width comparable to the layer depth will grow exponentially with the shortest time scale and will quickly come to dominate. As a result, the buoyant layer will form into a series of rising blobs with a spacing of about $2w$.

Now let us consider the particular situation in which the density difference is due to the lower layer having a higher temperature because the bottom boundary of the fluid is hot. Then the density difference would be $\Delta\rho = \rho\alpha\Delta T$, where $\Delta T$ is a measure of the average difference in temperature between the layers. Suppose first that the thermal conductivity of the fluid is high and the growth of the bulge is negligibly slow: then temperature differences would be quickly smeared out by thermal diffusion. In the process, the bulge would be smeared out. After a time the temperature would approach a uniform gradient between the bottom and top boundaries, and the bulge would have ceased to exist.

However, I showed above that the bulge grows because of its buoyancy. Evidently there is a competition between the buoyancy and the thermal diffusion. We can characterise this competition in terms of the time scales of the two processes: $\tau_{RT}$ for the buoyant growth and $\tau_\kappa$ for the thermal diffusion, where

$$\tau_\kappa = D^2/\kappa \tag{8.4.7}$$

We can use $D$ as a measure of the distance that heat must diffuse in order to wipe out the fastest growing bulge. In order for the bulge to grow, $\tau_{RT}$ will need to be significantly less than $\tau_\kappa$. From Equations (8.4.6) and (8.4.7), this condition is

$$\frac{g\Delta\rho D^3}{\kappa\mu} = Ra \geq c \tag{8.4.8}$$

where $c$ is a numerical constant and you can recognise the left-hand side of Equation (8.4.8) as the Rayleigh number.

This result tells us that there is indeed a value of the Rayleigh number that must be exceeded before the thermal boundary layer can rise unstably in the presence of continuous heat loss by thermal diffusion. If it cannot, there will be no thermal convection. Thus we

have derived the essence of Rayleigh's result. In this case, we do not get a very good numerical estimate of the critical value of the Rayleigh number, since a rigorous stability analysis yields $c \approx 1000$, rather than $c \approx 1$.

The quantitative value may not be very accurate, but we have been able to see that the controlling physics is the competition between the Rayleigh–Taylor instability and thermal diffusion (the Rayleigh–Taylor instability involving an ever-changing balance between buoyancy and viscous resistance). In fact, you can see now that the Rayleigh number is just the ratio of the time scales of these two processes:

$$Ra = \frac{\tau_\kappa}{\tau_{\mathrm{RT}}} \tag{8.4.9}$$

The mantle Rayleigh number is at least $3 \times 10^6$, well above the critical value of about 1000. This indicates that the mantle is well beyond the regime of marginal stability. One way to look at this, using Equation (8.4.9), is that the thermal diffusion time scale is very long, which means that heat does not diffuse very far in the time it takes the fluid to become unstable and overturn. This means that the thermal boundary layers will be thin compared with the fluid layer thickness.

Thin boundary layers were assumed without comment in the simple theory of convection given in Section 8.2. That theory actually is most appropriate with very thin boundary layers, that is at very high Rayleigh numbers. For this reason it is known as the boundary layer theory of convection. Thus the marginal stability theory applies just above the critical Rayleigh number, while the boundary layer theory applies at the other extreme of high Rayleigh number.

## 8.5 Flow patterns

In a series of classic experiments, Benard [5] observed that, in a liquid just above marginal stability, the convection flow formed a system of hexagonal cells, like honeycomb, when viewed from above. Considerable mathematical effort was devoted subsequently to trying to explain this. It was presumed that it must imply that hexagonal cells are the most efficient at convecting heat. It turned out that the explanation for the hexagons lay in the effect of surface tension in the experiments, and specifically on differences in surface tension accompanying differences in temperature. Surface tension

was important because Benard's liquid layers were only 1 mm or less in thickness.

There is an important lesson here. If a factor like the temperature-dependence of surface tension could so strongly influence the horizontal pattern, or 'planform', of the convection, then the fluid must not have a strong preference for a particular planform; that is, different planforms must not have much influence on the efficiency of the convection. The implication is that, in other situations, other factors influencing the material properties of the fluid in the boundary layers might also have a strong influence on planform.

Pursuing this logic, if the top and bottom thermal boundary layers in a fluid layer should have material properties that are distinctly different from each other, then each may tend to drive a distinctive pattern of convection. What then will be the resulting behaviour? The possibility of the different thermal boundary layers tending to have different planforms is not made obvious in standard treatments of convection. Whether it occurs depends both on the physical properties of the fluid and on the mode of heating, which we will look at next.

In the mantle, a hot boundary layer does have distinctly different mechanical properties from a cold boundary layer, and the two seem to behave quite differently. As well, the cold boundary layer in the earth is laterally heterogeneous, containing continents and so on, and it develops other heterogeneities in response to deformation: it breaks along faults. The effects of material properties on flow patterns are major themes of the next three chapters, which focus on the particular case of the earth's mantle.

## 8.6 Heating modes and thermal boundary layers

Textbook examples of convection often show the case of a layer of fluid heated from below and cooled from above. In this case there is a hot thermal boundary layer at the bottom and a cool thermal boundary layer at the top (Figure 8.3a). If, as well, the Rayleigh number is not very high, the resulting pattern of flow is such that each of the thermal boundary layers reinforces the flow driven by the other one. In other words the buoyant upwellings rise between the cool downwellings, so that a series of rotating 'cells' is formed which are driven in the same sense of rotation from both sides. This cooperation between the upwellings and downwellings disguises the fact that the boundary layers are dynamically separate entities. It is possible that they might drive different flow patterns, as I intimated in the last section. It is also possible that one of the thermal boundary layers is weak or absent.

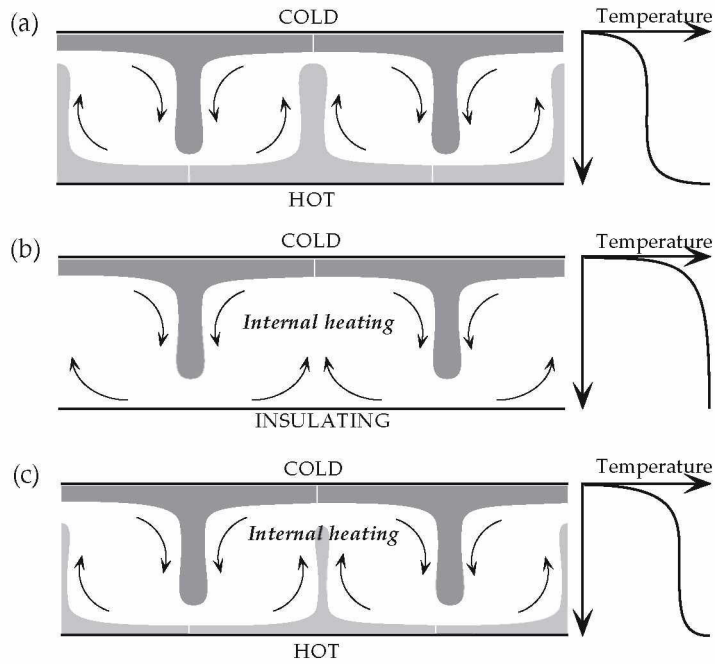


Figure 8.3. Sketches illustrating how the existence and strength of a lower thermal boundary layer depend on the way in which the fluid layer is heated.

For example, a fluid layer might be heated from within by radioactivity. If there is no heat entering the base, perhaps because it is insulating, then there will be no hot thermal boundary at the bottom. If the fluid layer is still cooled from the top, the only thermal boundary layer will be the cool one at the top (Figure 8.3b). In fact this was assumed, without comment, in the simple theory of convection presented in Section 8.2. In this case, the cool fluid sinking from the top boundary layer still drives circulation, but the *upwelling* is *passive*. By this I mean that although the fluid flows upwards between the downwellings (Figure 8.3b), it is not buoyant relative to the well-mixed interior fluid. It is merely being displaced to make way for the actively sinking cold fluid.

Although this may seem to be a trivial point here, it has been very commonly assumed, for example, that because there is clearly upwelling occurring under midocean ridges, the upwelling mantle material is hotter than normal and thus buoyant and 'actively' upwelling. We will see evidence in Chapter 10 that this is usually not true. A lot of confusion about the relationship between mantle convection and continental drift and plate tectonics can be avoided by keeping this simple point clearly in mind.

More generally, the heat input to the fluid layer might be a combination of heat entering from below and heat generated within (by radioactivity, in the case of the mantle), and states intermediate between those of Figures 8.3a and 8.3b will result (Figure 8.3c). Suppose, as implied in Figure 8.3a, that the temperature of the lower boundary is fixed. If there is no internal heating, then the temperature profile will be like that shown to the right of Figure 8.3a. If there is no heating from below, the internal temperature will be the same as the bottom boundary, as shown to the right of Figure 8.3b. If there is some internal heating, then the internal temperature will be intermediate, as in Figure 8.3c. As a result, the top thermal boundary layer will be stronger (having a larger temperature jump across it) and the lower thermal boundary layer will be correspondingly weaker. The mantle seems to be in such an intermediate state, as we will see.

The point is illustrated by numerical models in Figure 8.4. The left three panels are frames from a model with a prescribed bottom temperature and no internal heating. You can see both cool sinking columns and hot rising columns. The right three panels are from an internally heated model, and only the upper boundary layer exists. Downwellings are active, as in the bottom-heated model, but the upwellings are passive, broad and slow. Away from downwellings, isotherms are nearly horizontal, and the fluid is stably stratified. This is because the coolest fluid sinks to the bottom, and is then

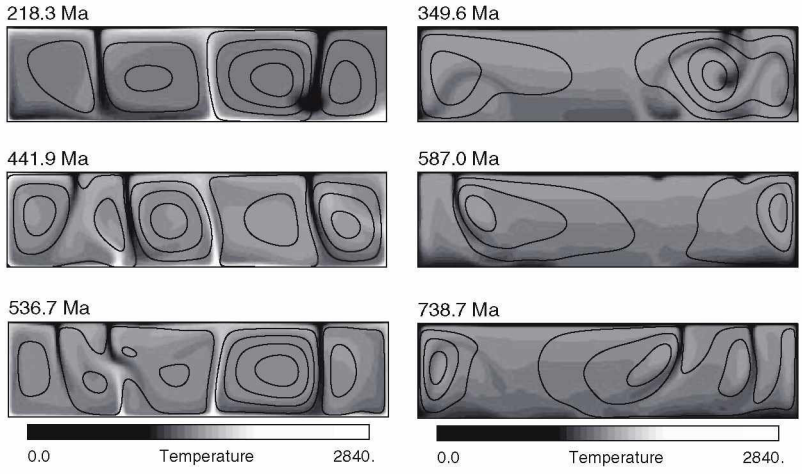


Figure 8.4. Frames from numerical models, illustrating the differences between convection in a layer heated from below (left-hand panels) and in a layer heated internally (right-hand panels). (Technical specifications of these models are given in Appendix 2.)

slowly displaced upwards by later cool fluid as it slowly warms by internal heating.

Figure 8.4 illustrates two other important points. First, the flow is unsteady. This is characteristic of convection at high Rayleigh numbers in constant-viscosity fluids. It is because the heating is so strong that the boundary layers become unstable before they have travelled a distance comparable to the depth of the fluid, which is the width of cells that allows the most vertical limbs while also minimising the viscous dissipation. Incipient instabilities in the top boundary layer are visible in the middle right panel of Figure 8.4. By the last panel they have developed into full downwellings.

Second, the two thermal boundary layers in the left sequence are behaving somewhat independently, especially on the left side of the panels. In fact in the bottom panel an upwelling and a downwelling are colliding. This illustrates the point made earlier that each boundary layer is an independent source of buoyancy, and they may interact only weakly. This becomes more pronounced at higher Rayleigh numbers.

### 8.6.1 Other Rayleigh numbers [*Advanced*]

We have so far specified the thermal state of the convecting fluid in terms of *temperatures* prescribed for each boundary. However, in Figures 8.3b and 8.4 (right panels) the bottom boundary is specified as *insulating*, that is as having zero heat flux through it, and the heating is specified as being internal. The temperature is not specified ahead of time. It is evident that this model is specified in terms of heat input, rather than in terms of a temperature difference between the boundaries. How then can the Rayleigh number be defined?

The philosophy of the dimensional estimates used in this chapter is that *representative* quantities are used. With appropriate choices, order-of-magnitude estimates will (usually) result. The Rayleigh number defined by Equation (8.3.2) is defined in terms of such representative quantities. This suggests that we look for *representative* and *convenient* measures in different situations.

We lack a representative temperature difference for the situation in Figure 8.3b, but we can assume that a heat flux, $q$, is specified. One way to proceed is to derive a quantity from $q$ that has the dimensions of temperature; for example, we can use the temperature difference, $\Delta T_q$, across the layer that would be required to *conduct* the specified heat flux, $q$:

$$\Delta T_q = qD/K$$

We can then define a new Rayleigh number as

$$R_q = \frac{g\rho\alpha D^3 \Delta T_q}{\kappa\mu} = \frac{g\rho\alpha q D^4}{K\kappa\mu} \tag{8.6.1}$$

This Rayleigh number is useful in any situation in which it is the heat input rather than a temperature difference that is specified.

It is possible in principle that some heat, say $q_b$, is specified at the base, and some is specified to be generated internally. If the internal heating is uniform, and generated at the rate $H$ per unit volume of fluid, then the rate of internal heat generation per unit area of the layer surface is $HD$. The total heat input will then be

$$q = q_b + HD$$

Although in a laboratory setting it is not easy to prescribe a heat flux, it is easy in numerical experiments and it is useful to make the conceptual distinction between the two kinds of bottom thermal boundary layer: prescribed temperature and prescribed heat flux.

The Rayleigh numbers $R_q$ (Equation (8.6.1)) and $Ra$ (Equation (8.3.2)) are distinct quantities with different numerical values, as we will see, and this is why different symbols are used here for them. However they are also related. Recall that the Nusselt number, $Nu$, was defined as the ratio of actual heat flux, $q$, to the heat flux, $q_K$, that would be conducted with the same temperature difference across the layer (Equation (8.3.10)). In the case considered earlier, it was $q_K$ that was specified ahead of time and $q$ that was determined by the behaviour of the fluid layer. Here it is the reverse. However we can still use this definition of $Nu$. Thus, if the actual temperature difference across the layer that results from the convection process is $\Delta T$, then $q_K = K\Delta T/D$ and

$$Nu = q/q_K = \Delta T_q/\Delta T \tag{8.6.2}$$

Thus here the Nusselt number gives the ratio of the temperature difference, $\Delta T_q$, that would be required to conduct the heat flux $q$ through the layer, to the actual temperature difference in the presence of convection.

Similarly, although $\Delta T$ is not known ahead of time here, it can still be used conceptually to define the Rayleigh number $Ra$ (Equation (8.3.2)). It is then easy to see the relationship between $Ra$ and $R_q$:

$$\frac{R_q}{Ra} = \frac{\Delta T_q}{\Delta T} = Nu \tag{8.6.3}$$

In the earlier discussion of scaling, we found that $Nu \sim Ra^{1/3}$, so $R_q \sim Ra^{4/3}$. Thus if $Ra$ has the value $3 \times 10^6$ estimated earlier, for example, then $R_q$ will be about $4.3 \times 10^8$. Thus $R_q$ is numerically larger than $Ra$. Nevertheless it is a convenient way to characterise cases where it is the heat flux that is specified, rather than the temperature difference. You must of course be careful about which definition of Rayleigh number is being used in a given context, as they have different scaling properties as well as different numerical values.

This discussion illustrates the general point that different Rayleigh numbers may be defined in different contexts. There is nothing profound about this, it is merely a matter of adopting a definition that is convenient and relevant for the context, so that it encapsulates the scaling properties of the particular situation.

For the earth's mantle, however, there is a complication. An appropriate way of specifying the heat input into models of the mantle is through a combination of internal heating from radioactivity and a prescribed temperature at the base. Although the value of the temperature at the base of the mantle is not well known, the liquid core is believed to have a low viscosity, so that it would keep the temperature quite homogeneous. This means the core can be viewed as a heat bath imposing a uniform temperature on the base of the mantle. This combination of a heating rate and a prescribed uniform bottom temperature is not covered by either of the Rayleigh numbers $Ra$ or $R_q$, so there is not a convenient a priori thermal prescription of mantle models. In the mantle it is the heat *output*, at the top surface that is well-constrained. This means that some trial and error may be necessary to obtain models that match the observed heat output of the mantle.

## 8.7 Dimensionless equations [*Advanced*]

The equations governing convection are often put into dimensionless form, that is they are expressed in terms of dimensionless variables. This is done to take advantage of the kind of scaling properties that we have been looking at, because one solution can then be scaled to a variety of contexts. There are different ways in which this can be done. We have seen an example of this already, in the different Rayleigh numbers that can be defined, depending on the way the fluid is heated. Other alternatives are more arbitrary. For example, two different time scales are com-

monly invoked, and others are possible. Since these alternatives are not usually presented systematically, I will do so here.

The equations governing the flow of a viscous incompressible fluid were developed in Chapter 6 (Equation (6.6.3)), and the equation governing heat flow with advection, diffusion and internal heat generation was developed in Chapter 7 (Equation (7.8.2)). The following dimensional forms of these equations are convenient here.

$$\frac{\partial \tau_{ij}}{\partial x_j} - \frac{\partial P}{\partial x_i} = -B_i = \rho g_i \tag{8.7.1}$$

$$\frac{\mathrm{D}T}{\mathrm{D}t} \equiv \frac{\partial T}{\partial t} + v_i \frac{\partial T}{\partial x_i} = \kappa \nabla^2 T + \frac{A}{\rho C_P} \tag{8.7.2}$$

In Equation (8.7.1), the buoyancy force $B_i$ (positive upwards), is written in terms of the density and the gravity vector $g_i$ (positive downwards). In Equation (8.7.2), the first derivative, $\mathrm{D}T/\mathrm{D}t$, is known as the total derivative, and its definition is implicit in the first identity of that equation. $A$ is the internal heat production per unit time, per unit volume.

Three scaling quantities suffice to express these equations in dimensionless form: a length, a temperature difference and a time. For length, an appropriate choice is usually $D$, the depth of the convection fluid layer. Using this, we can define dimensionless position coordinates, $x_i$, for example, such that

$$x_i' = Dx_i$$

where I have *changed notation*: the prime denotes a dimensional quantity and unprimed quantities are dimensionless, unless specifically identified as a dimensional scaling quantity, like $D$.

For temperature, we have seen in the last section two possible choices:

$$\Delta T = \Delta T_T = (T_\mathrm{b} - T_\mathrm{s}) \tag{8.7.3}$$

$$\Delta T = \Delta T_q = qD/K \tag{8.7.4}$$

For the moment, I will retain the general notation $\Delta T$ to cover both of these possibilities.

A time scale that is often used is the thermal diffusion time scale of Equation (8.3.6): $t_\kappa = D^2/\kappa$. Another one sometimes used is

$t_\kappa/Ra$. A third possibility emerged from the earlier discussion of scaling, namely the transit time $t_v = t_\kappa/Ra^{2/3}$ (Equations (8.3.7), (8.3.8)). Here I will carry all three possibilities by using a general time scale $t_n$, where

$$\begin{aligned} t_1 &= t_\kappa = D^2/\kappa \\ t_2 &= t_\kappa/Ra \\ t_3 &= t_v = t_\kappa/Ra^{2/3} \end{aligned} \tag{8.7.5}$$

Dimensional scales can be derived from $D$, $\Delta T$ and $t_n$ for viscous stress, buoyancy and heat generation rate as follows. Viscous stress is viscosity times velocity gradient, so an appropriate scale is $\mu(D/t_n)/D = \mu/t_n$. Buoyancy per unit volume is $g\Delta\rho = g\rho_0\alpha\Delta T$. Using these scales in Equation (8.7.1) yields

$$\frac{\mu}{Dt_n}\left(\frac{\partial\tau_{ij}}{\partial x_j} - \frac{\partial P}{\partial x_i}\right) = g\Delta\rho(\rho g_i)$$

that is

$$\frac{\partial\tau_{ij}}{\partial x_j} - \frac{\partial P}{\partial x_i} = R_{\mathrm{F}}(\rho g_i) \tag{8.7.6}$$

where $R_{\mathrm{F}}$ denotes a dimensionless combination of constants in the force balance equations:

$$R_{\mathrm{F}} = \frac{g\Delta\rho D t_n}{\mu} \tag{8.7.7}$$

Similarly, for Equation (8.7.2) we need a scale for heat generation. The heat flux scale identified earlier (Equations (8.3.9) and (8.3.10)) is $q_K$, the heat flux that would be conducted with the same temperature difference. The heat generation rate per unit volume that corresponds to this is $q_K/D = K\Delta T/D^2$. Then Equation (8.7.2) becomes

$$\frac{\Delta T}{t_n}\left(\frac{\mathrm{D}T}{\mathrm{D}t}\right) = \frac{\kappa\Delta T}{D^2}\left(\nabla^2 T\right) + \left(\frac{K\Delta T}{\rho C_P D^2}\right)A$$

Remembering that $K/\rho C_P = \kappa$, this can be written

$$\frac{\mathrm{D}T}{\mathrm{D}t} = R_{\mathrm{H}}\left(\nabla^2 T + A\right) \tag{8.7.8}$$

where $R_H$ denotes a dimensionless combination in the heat equation:

$$R_H = \frac{\kappa t_n}{D^2} \tag{8.7.9}$$

Equations (8.7.6) and (8.7.8) are dimensionless versions of the flow and heat equations, and they involve the two dimensionless ratios $R_F$ and $R_H$. The three choices of time scale proposed in Equations (8.7.5) then yield

$$t_n = t_1 : \qquad R_F = Ra \qquad R_H = 1 \tag{8.7.10a}$$

$$t_n = t_2 : \qquad R_F = 1 \qquad R_H = 1/Ra \tag{8.7.10b}$$

$$t_n = t_3 : \qquad R_F = Ra^{1/3} \quad R_H = 1/Ra^{2/3} \tag{8.7.10c}$$

The choice of time scale is mainly a matter of convenience. With the choice $t_3$, one dimensionless time unit will correspond approximately with a transit time, regardless of the Rayleigh number, and it will be easier to judge the progress of a numerical calculation. On the other hand, the choice between $\Delta T_T$ and $\Delta T_q$ depends on the mode of heating of the fluid. The notation thus refers to a more substantial difference in the model than convenience, and more care must be taken to ensure the proper interpretation of results of calculations.

## 8.8 Topography generated by convection

The topography generated by convection is of crucial importance to understanding mantle convection, since the earth's topography provides some of the most important constraints on mantle convection. Here I present the general principle qualitatively. The particular features of topography to be expected for mantle convection, and their quantification and comparison with observations, will be given in following Chapters. We have already covered one important example in Chapter 7, the subsidence of the sea floor.

The central idea is that buoyancy does two things: it drives convective flow and it vertically deflects the horizontal surfaces of the fluid layer. Because the buoyancy is (in the thermal convection of most interest here) of thermal origin, there are intimate relationships between topography, fluid flow rates and heat transport rates.

The principle is illustrated in Figure 8.5. This shows a fluid layer with three buoyant blobs, labelled (a), (b) and (c). Blob (a) is close to the top surface and has lifted the surface. The surface uplift is required by Newton's laws of motion. If there were no force opposing the buoyancy of the blob, the blob would continuously accelerate. Of course there are viscous stresses opposing the blob locally, but these only shift the problem. The fluid adjacent to the blob opposes the blob, but then this fluid exerts a force on fluid further out. In other words, the viscous stresses *transmit* the force through the fluid, but do not result in any net opposing force. This comes from the deflected surface.

There is, in Figure 8.5, blob (a), a simple force balance: the weight of the topography balances the buoyancy of the blob. Geologists might recognise this as an *isostatic* balance. Another way to think of it is that the topography has negative buoyancy, due to its higher density than the material it has displaced (air or water, in the case of the mantle). Recalling the definition of buoyancy given earlier (Equation (8.1.1)), this implies that the excess mass of the topography equals the mass deficiency of the blob.

As I have already stressed, there is in this very viscous system an *instantaneous* force balance, even though the blob is moving. Such topography has sometimes been referred to as 'dynamic topography', but this terminology may be confusing, because it may suggest that momentum is involved. It is not. The balance is a static (strictly, a quasi-static), instantaneous balance. The 'dynamic' terminology derives from the term 'dynamic stresses', which means the stresses due to the motion, which are the viscous stresses. While this terminology may be technically correct, it is not very helpful, because it may obscure the fact that there is a simple force balance

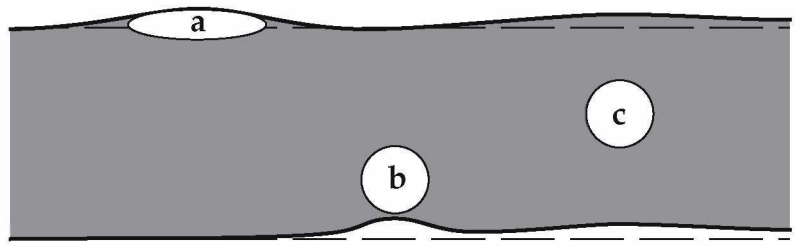


Figure 8.5. Sketch of the effects of buoyant blobs on the surfaces of a fluid layer. The layer surfaces are assumed to be free to deflect vertically, with a less dense fluid (e.g. air or water) above, and a more dense fluid (e.g. the core) below.

involved, and it may make the problem seem more complicated than it really is.

Blob (b) in Figure 8.5 is near the bottom of the fluid layer. It causes the bottom surface of the fluid to deflect. This is because the viscous stresses caused by the blob are larger close to the blob than far away, so the main effect is on the nearby bottom surface. I have implicitly assumed in Figure 8.5 that there is a denser fluid below the bottom surface, such as the core under the mantle. In this case, the topography causes denser (core) material to replace less dense (mantle) material. Thus it generates a downward compensating force, or negative buoyancy, just as does topography on the top surface. This force balances the buoyancy of blob (b).

Does blob (b) cause any deflection of the top surface? Yes, there will be a small deflection over a wide area of the surface. Blob (c) makes this point more explicitly: it is near the middle of the layer, and it deflects both the top and the bottom surfaces by similar amounts. In this case, we can see that the force balance is actually between the positive buoyancy of the blob and the *two* deflected surfaces. In fact this will always be true, even for blobs (a) and (b), but I depicted them close to one surface or the other to simplify the initial discussion, since this makes the deflection of one surface negligible.

To summarise the principle, buoyancy in a fluid layer deflects both the top and the bottom surfaces of the fluid (supposing they are deformable), and the combined weight of the topographies balances the internal buoyancy. The amount of deflection of each surface depends on the magnitude of the viscous stresses transmitted to each surface. This depends on the distance from the buoyancy to the surface. It also depends on the viscosity of the intervening fluid, a point that will be significant in following chapters.

Now apply these ideas to the thermal boundary layers we were considering above. The top thermal boundary layer is cooler and denser than the ambient interior fluid, so it is negatively buoyant and pulls the surfaces down. Because it is adjacent to the top fluid surface, it is this surface that is deflected the most. There will be, to a good approximation, an isostatic balance between the mass excess of the thermal boundary layer and the mass deficiency of the depression it causes. The result is sketched in Figure 8.6 in a form that is like that of the mantle. The topography on the left is highest where the boundary layer is thinnest. Away from this in both directions, the surface is depressed by the thicker boundary layer.

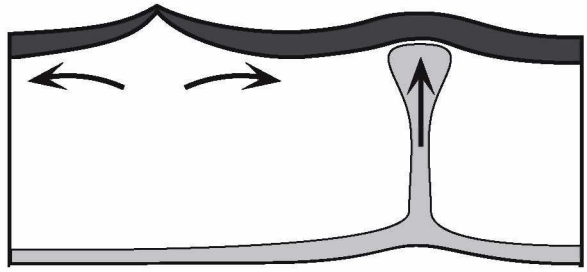

Figure 8.6. Sketch of two types of topography on the top surface of a convecting fluid layer. The top thermal boundary layer cools, thickens and subsides by thermal contraction as it moves away from the spreading centre at left, leaving a topographic high where it is thin. The bottom thermal boundary layer generates no topography on the top surface until material from it rises to the top, where it raises the top surface (upwelling on right).

On the other hand, the bottom thermal boundary layer is adjacent to the bottom surface of the fluid, and generates topography there (Figure 8.6). It does not generate significant topography on the top surface except where a buoyant column has risen to the top of the fluid layer. There the top surface is lifted. Thus it is possible for the bottom thermal boundary layer to generate topography on the top surface, but only after material from it has risen to the top.

There is an important difference between the two topographic highs in Figure 8.6. The high on the left has no 'active' upwelling beneath it: it is high because the surface on either side of it has subsided, because of the negative buoyancy of the top thermal boundary layer. In contrast, the high on the right does have an 'active', positively buoyant upwelling beneath it that has lifted it up.

You will see in the following chapters that the forms of convection driven by the two mantle boundary layers are different. As a result, the forms of topography they generate are recognisably different. Because buoyancy is directly involved both in the topography and in the convection, the observed topography of the earth contains important information about the forms of convection present in the mantle.

Even better, the topography contains *quantitative* information about the fluxes of buoyancy and heat involved. This is most readily brought out in the mantle context, where the topographic forms are distinct and lend themselves to extracting this information. However, it should by now be no surprise to you that such information is present, given the intimate involvement of buoyancy, convection and topography.

## 8.9 References

1. D. L. Turcotte and E. R. Oxburgh, Finite amplitude convection cells and continental drift, *J. Fluid Mech.* **28**, 29–42, 1967.
2. D. L. Turcotte and G. Schubert, *Geodynamics: Applications of Continuum Physics to Geological Problems*, 450 pp., Wiley, New York, 1982.
3. Lord Rayleigh, On convective currents in a horizontal layer of fluid when the higher temperature is on the under side, *Philos. Mag.* **32**, 529–46, 1916.
4. S. Chandrasekhar, *Hydrodynamic and Hydromagnetic Stability*, Oxford University Press, Oxford, 1961.
5. H. Benard, Les tourbillons cellulaires dans une nappe liquide transportant de la chaleur par convection en régime permanent, *Ann. Chim. Phys.* **23**, 62–144, 1901.

## 8.10 Exercises

1. Use Equations (8.1.1) and (8.1.2) to evaluate the buoyancy of the following. These are meant to be rough estimates, so do not calculate results to more than one or two significant figures.
   (a) A ball bearing 1 cm in diameter and with density 7.7 $Mg/m^3$ in mantle of density 3.3 $Mg/m^3$.
   (b) A plume head with a radius of 500 km and temperature excess of 300 °C in a mantle of density 3.3 $Mg/m^3$ and thermal expansion coefficient $3 \times 10^{-5}$/°C.
   (c) A sheet of subducted lithosphere 100 km thick extending to a depth of (i) 600 km, (ii) 3000 km. Calculate a buoyancy per metre in the horizontal direction of the oceanic trench. Assume the slab temperature varies linearly through its thickness from 0 °C to the mantle temperature of 1300 °C; you need only consider its mean temperature deficit. Assume other parameters as above.
   (d) Suppose part of the slab just considered included oceanic crust 7 km thick with a density in the mantle of 3.2 $Mg/m^3$. Calculate its contribution to the slab buoyancy.

2. Repeat the derivation of the approximate formula (8.2.5) for the convection velocity in the model of Figure 8.1, but this time assume that the cell length, $L$, is not the same as its depth, $D$. You will need to consider the horizontal and vertical velocities, $u$ and $v$, to be different, and to relate them using conservation of mass. You will also need to include two terms in the viscous resistance, one

proportional to the velocity gradient $2u/D$ and one proportional to $2v/L$. The answer can be expressed in the form of Equation (8.2.5) with the addition of a factor involving $(L/D)$. Using values from the text, compare the velocity when $L = D = 3000\,\text{km}$ and when $L = 14\,000\,\text{km}$, the maximum width of the Pacific plate.